

Cold and dense cesium clouds in far-detuned dipole traps

D. Boiron,¹ A. Michaud,¹ J. M. Fournier,² L. Simard,¹ M. Sprenger,³ G. Grynberg,¹ and C. Salomon¹¹Laboratoire Kastler Brossel and Collège de France, 24 rue Lhomond, 75231 Paris, France²Rowland Institute for Science, 100 Edwin H. Land Boulevard, Cambridge, Massachusetts 02142³Fakultät für Physik, Universität Konstanz, D-78457 Konstanz, Germany

(Received 4 November 1997)

We study the behavior of cesium atoms confined in far-detuned laser traps and submitted to blue Sisyphus cooling. First, in a single focused yttrium aluminum garnet (YAG) beam, the atomic cloud has a rod shape with a $6\text{-}\mu\text{m}$ transverse waist radius, a temperature of $2\text{ }\mu\text{K}$, and a transient density of $10^{12}\text{ atoms/cm}^3$. For this sample, we have not detected any influence of photon multiple scattering on the atomic temperature, in contrast to previous measurements in *isotropic* samples. Second, the YAG laser is used to produce a $29\text{-}\mu\text{m}$ period hexagonal optical lattice in which we directly observe the localization of the atoms by absorption imaging. Equilibrium densities on the order of $10^{13}\text{ atoms/cm}^3$ are achieved in this structure. [S1050-2947(98)50706-8]

PACS number(s): 32.80.Pj

Atom manipulation using laser light has experienced a rapid growth in the recent years [1]. Laser-cooled and/or laser trapped atoms are used in a variety of applications such as cesium fountain clocks, atom interferometry, atom lithography, atom guiding in optical fibers, and the production of Bose-Einstein condensates. This manipulation can be dissipative, such as in magneto-optical traps (MOT's), optical molasses, and lattices where confinement and cooling are simultaneously present but where the density is limited to about $10^{11}\text{ atoms/cm}^3$. On the other hand, the use of far-detuned dipole traps leads to nearly nondissipative potentials with very low spontaneous emission rates ($\lesssim 1\text{ s}^{-1}$) in which precooled atoms can be trapped [2–4]. Raman cooling in such traps has been performed for Na atoms leading to a temperature of $1\text{ }\mu\text{K}$ at a density of $4 \times 10^{11}\text{ atoms/cm}^3$ [5] and for cesium atoms to $2\text{ }\mu\text{K}$ and $1.3 \times 10^{12}\text{ atoms/cm}^3$ [6]. In both experiments the size of the atomic cloud was in the $10\text{--}100\text{ }\mu\text{m}$ range. The loading of the dipole trap may also be produced by adiabatic transfer from a superimposed nearly resonant molasses [7]. We present here another scheme for producing dense and confined samples. This scheme is very simple and it produces extremely small (micrometer range) and dense ($\sim 10^{13}\text{ atoms/cm}^3$) cesium samples. It relies on the addition of blue Sisyphus cooling (BSC) to far-red-detuned dipole traps. This BSC cooling (also called gray molasses) uses a $F_g \rightarrow F_e = F_g - 1$ transition and a positive laser detuning ($\omega_L > \omega_{\text{at}}$). It provides cesium atoms in states of the $F_g = 3$ hyperfine level that are only weakly coupled to the cooling light field, and the minimum temperature at low density is $1\text{ }\mu\text{K}$, three times lower than the temperature in ordinary red-detuned optical molasses or MOTs [8]. We show here that this cooling is very efficient in far-detuned traps. It leads to high densities that are not limited by hyperfine changing collisions and it offers the advantage over the Raman cooling scheme that it does not require any additional laser. We have investigated first the simple case of a single focused yttrium aluminum garnet (YAG) beam. Because of the quasi-unidimensional geometry, we have not detected any influence of photon multiple scattering on the atomic temperature at the $0.5\text{-}\mu\text{K}$ level. This result constitutes an important step on the way to reaching quantum

degeneracy by purely optical methods. Then the same YAG laser is used to produce a two-dimensional hexagonal optical lattice in which $10\text{-}\mu\text{K}$ atoms are arranged in rods having a $3.5\text{-}\mu\text{m}$ waist radius, a $29\text{-}\mu\text{m}$ spacing, each containing about 10^4 atoms. We have taken absorption images that directly display the periodic ordering of the atoms in this optical structure and we show that three-dimensional (3D) trapping is obtained by means of the Talbot effect [9].

As a first test of the efficiency of the BSC in a far-detuned trap, we focus a TEM_{00} YAG laser (at $1.06\text{ }\mu\text{m}$) onto the cloud of a cesium magneto-optical trap produced in a low vapor pressure cell [Fig. 1, path (a)]. The YAG beam is horizontal and has a waist of $w_0 = 45\text{ }\mu\text{m}$.

In the absence of the MOT and of the BSC, the potential acting on the atoms is the sum of the dipole potential of the YAG beam and of the gravitational potential. Because the confocal parameter $b = kw_0^2 \approx 1.2\text{ cm} \gg w_0$, the trapping force along the YAG beam is much weaker than in the trans-

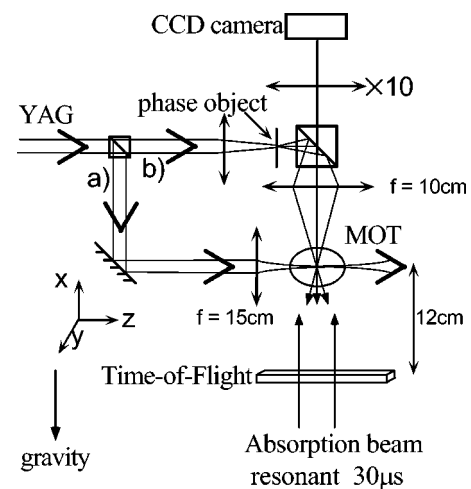


FIG. 1. Experimental setup. The YAG beam creates a horizontal dipole trap, path (a), or an optical lattice, path (b). Absorption images are taken with a vertical pulsed beam and are magnified by a $\times 10$ microscope objective. (a) The YAG power is 700 mW and the waist is $45\text{ }\mu\text{m}$. (b) Trapping in optical lattices. The YAG beam images a periodic pattern onto the atomic sample.

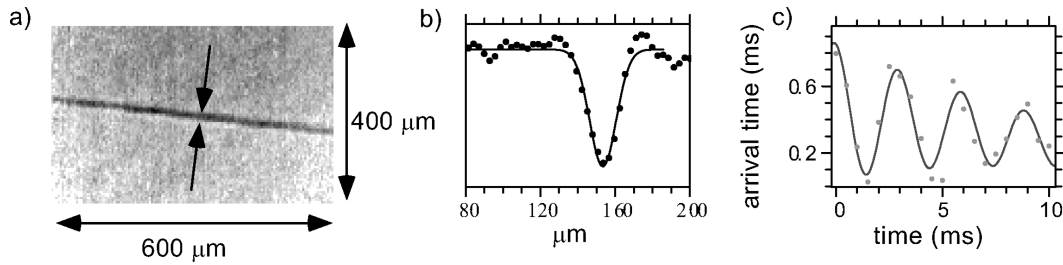


FIG. 2. (a) Absorption image of cesium atoms trapped in a single beam dipole trap. (b) Section of (a); the rms size is $6.0 \mu\text{m}$. (c) Measurement of the vertical oscillation frequency (see text): the YAG trap is interrupted for ~ 1 ms and turned on again for an adjustable time (horizontal axis). Vertical axis: mean arrival time of the atoms in the TOF probe beam. Here $\Omega_x/2\pi = 330$ Hz.

verse direction. For a linear polarization, the depth U_0 of the dipole potential is the same for all Zeeman sublevels and is equal to $\hbar\Omega_R^2/4\delta_{\text{eff}}$, where Ω_R is the peak Rabi frequency, and δ_{eff} is an effective detuning given by $1/\delta_{\text{eff}} = 1/3\delta_1 + 2/3\delta_2$. $\delta_1 = 2\pi \cdot 5.3 \times 10^{13}$ rad/s (respectively, $\delta_2 = 2\pi \cdot 7.0 \times 10^{13}$ rad/s) is the detuning between the YAG laser and the first D1 line (respectively, D2) of cesium. The quantity $\eta = mgw_0/U_0$ characterizes the drop of potential due to gravity on the typical size w_0 as compared to U_0 . In order to have stable trapping against gravity one should have $\eta \ll 1$. The effect of gravity is then only a mere shift of the minimum of the potential with a negligible modification of the potential depth and of the oscillation frequency at the bottom of the trap $\Omega_{\text{osc}} = (4U_0/mw_0^2)^{1/2}$. Typical values are $P = 700$ mW, $U_0/k_B = 50 \mu\text{K}$, $\eta = 0.13$, and $\Omega_{\text{osc}} = 2\pi \cdot 390$ rad/s. Because of the very large detuning of the YAG laser, the photon scattering rate is only 2 s^{-1} .

In order to load this trap, we first capture about 3×10^7 atoms in a MOT for 1 s while having the YAG beam continuously on. The intensity of the MOT beams is then reduced during 30 ms to contract the atomic cloud to a peak density of 5×10^{10} atoms/cm³ and temperature of $30 \mu\text{K}$. By a simple shift of the distributed Bragg reflector laser frequencies (via the diode current), we further apply a blue Sisyphus cooling phase with the $F_g = 3 \rightarrow F_e = 2$ component of the D2 line with a laser detuning of $+5\Gamma$, where $\Gamma = 2\pi \times 5.3$ MHz is the natural width of the $P_{3/2}$ state. The MOT laser now serves as a repumping laser and is tuned to the $F_g = 4 \rightarrow F_e = 4$ transition. This accumulates atoms in nearly dark states of $F_g = 3$ with a temperature typically three times lower than in conventional red-detuned optical molasses [8]. During this cooling phase, which lasts about 30 ms, part of the atoms are dragged by the YAG potential toward the bottom of the YAG trap. After switching off the BSC, only these atoms remain trapped for much longer times.

The size of the atomic cloud is measured by an absorption imaging technique [10]. A 1-mm-diam probe beam resonant on the $F_g = 4 \rightarrow F_e = 5$ transition is sent vertically through the sample and its intensity distribution is recorded on a charge-coupled-device (CCD) camera. A lens with a 100-mm focal length at a distance of 200 mm from the trap makes an image with a $\times 1$ magnification of the trap outside the vacuum chamber with a numerical aperture of 0.1. A $\times 5$ or a $\times 10$ microscope objective enlarges the image on a CCD camera with a pixel size of $15 \mu\text{m}$. With this magnification, the rescaled pixel size is $3 \mu\text{m}$ ($1.5 \mu\text{m}$) for the $\times 5$ objective ($\times 10$) and is usually smaller than the images of the

distribution of trapped atoms. In order to have an instant picture of the atoms, the probe beam is pulsed for $\sim 30 \mu\text{s}$ and its intensity is close to the saturation intensity. If the atoms are in the $F_g = 3$ hyperfine level, a repumping pulse ($100 \mu\text{s}$) of resonant light on $F_g = 3 \rightarrow F_g = 3$ is applied to transfer the atoms from $F_g = 3$ to $F_g = 4$.

The temperature and number of cooled atoms in the YAG trap (or MOT) are measured by a standard time-of-flight (TOF) technique. After switching off suddenly the YAG beam, the atoms fall through a 1-mm-high probe beam located 12 cm below the trap. The probe contains two frequencies, one resonant with the $F_g = 4 \rightarrow F_e = 5$ cycling transition, and one resonant with the $F_g = 3 \rightarrow F_e = 3$ transition to detect atoms in $F_g = 4$ or $F_g = 3$. The atomic fluorescence is collected on a low noise photodiode. The temperature of the atoms along the vertical is deduced from the width of the time-of-flight peak and the number of atoms by its area. In order to distinguish the atoms trapped in the YAG beam from those that are only sustained by the BSC, we switch off the YAG laser a time τ_{YAG} after the BSC lasers are turned off. The TOF contains then two peaks (separated by τ_{YAG}), one associated with the atoms in the BSC and one associated with the trapped atoms.

The efficiency of the loading of the dipole trap as a function of the duration τ_{BSC} of the BSC phase passes through an optimum for $\tau_{\text{BSC}} = 30$ ms. The atom number in the YAG trap is then 2×10^5 atoms (3.7 % of the atoms in the BSC molasses), a factor of 4 higher than at short times. The temperature of the atoms in the YAG trap and in the BSC are the same to within $1 \mu\text{K}$. They range between 1 and $3 \mu\text{K}$, depending on the BSC parameters. This demonstrates that the cooling mechanism involved in BSC is not perturbed by the YAG potential. With traditional $F_g = 4$ to $F_g = 5$ molasses, the number of trapped atoms is 5 to 10 times smaller. The CCD camera image recorded at the optimum ($\tau_{\text{BSC}} = 30$ ms, $\tau_{\text{YAG}} = 30$ ms) is presented in Fig. 2.

As expected, the atom cloud has a rod shape. Its transverse size is well fitted by a Gaussian with rms radius $\sigma_y = 6_{-2}^{+1} \mu\text{m}$. The longitudinal size is $\sigma_z = 300 \mu\text{m}$. The corresponding peak atomic density $n = N/(2\pi)^{3/2}\sigma_x\sigma_y\sigma_z$ is $\sim 1 \times 10^{12}$ atoms/cm³ with a global uncertainty of about a factor of 3. In these conditions the measured temperature T is $2.0(5) \mu\text{K}$. Note that this density is a transient density because, in the longitudinal axis, the oscillation frequency being only 1.8 Hz, the sample has not reached its thermal equilibrium value of $950 \mu\text{m}$. In order to compare the observed size with theory, we measure the radial oscillation frequency as follows. We switch off the YAG beam for a short time

(~ 1 ms), during which the atoms acquire by gravity a common vertical velocity $v_x \sim 1$ cm/s. When the YAG beam is turned on again the cloud oscillates with a frequency Ω_x . Switching off again the YAG beam after a variable delay gives access to v_x through the mean arrival time of the atoms in the probe beam of the TOF detection. From Fig. 2, we obtain $\Omega_{\text{osc}}^{(\text{expt})}/2\pi = 330(30)$ Hz. This frequency is in reasonable agreement with the calculated one $390(120)$ Hz. For a harmonic potential, one has at thermal equilibrium

$$1/2k_B T = 1/2m\Omega_x^2 \sigma_x^2, \text{ i.e., } \sigma_x = v_x^{\text{rms}}/\Omega_x. \quad (1)$$

Therefore one expects $\sigma_x^{(\text{expt})} = 4.8(7)$ μm . This value is also in good agreement with the value deduced from the image $\sigma_y = 6_{-2}^{+1}$ μm , assuming cylindrical symmetry, and considering the finite resolution ($\sigma_{\text{res}} \sim 2.5$ μm) of our imaging system.

These data exhibit an interesting effect: our previous measurements on isotropic clouds of atoms in BSC with a rms radius of 700 μm showed a clear dependence of the temperature on the density, varying as $T = 1 + 0.6n/10^{10}$, where T is in μK and n in atoms/ cm^3 [8]. This effect was attributed to photon multiple scattering within the cold-atom cloud. Consequently, in the present high-density YAG trap ($n = 10^{12}$ atoms/ cm^3) we could expect a temperature of ~ 60 μK , 30 times higher than what we actually measure. We believe that this large difference is due to the geometry of our atomic sample. In a simple model, the temperature increase is proportional to the photon density n_ν within the cloud. n_ν results from a balance between the number of emitted photons that is proportional to the number of atoms nV (where V is the trap or molasses volume) and the photon escape proportional to the surface S of the trap. Because $V/S \sim R$ for a sphere of radius R and $V/S \sim r$ for a cylinder having a radius r much smaller than its height, we expect that at a given atomic density the excess temperature in the cylindrical geometry is reduced by a factor on the order of R/r , typically 10^2 , as compared to our previous spherical geometry. In this cylindrical geometry the expected slope dT/dn is thus $10^{-9} r$ cm^2 μK [Eq. (1)], where $r \sim \sigma_y$ is in centimeters. For $r = 6$ μm and $n = 10^{12}$ atoms/ cm^3 , we find $\delta T = 0.6$ μK , which is on the order of our experimental detectivity.

For the trapping experiments using optical lattice potentials, we use the optics described in Fig. 1, path (b). The YAG beam images a phase grating on the atomic cloud with a $f = 100$ mm lens, also used for the absorption imaging beam. With this method, arbitrary intensity patterns can be reproduced on the atoms. The grating is hexagonal with a period $p = 29$ μm and is illuminated over a waist of 140 μm by 2.5 W of the linearly polarized YAG beam. The power of the input beam is diffracted into a zeroth-order beam (power ratio, 0.07), six first-order beams (0.41), and 12 second-order beams (0.36). Higher orders ($N > 2$) are apertured by our optical system. These 19 beams are recombined and interfere in the image region to create a hexagonal two-dimensional (2D) optical potential. The loading of atoms in this periodic structure is the same as seen previously. Figure 3 is an absorption image taken just after having switched off the BSC beams. The atoms are trapped in periodically spaced sites in a hexagonal pattern of 29- μm periods. In

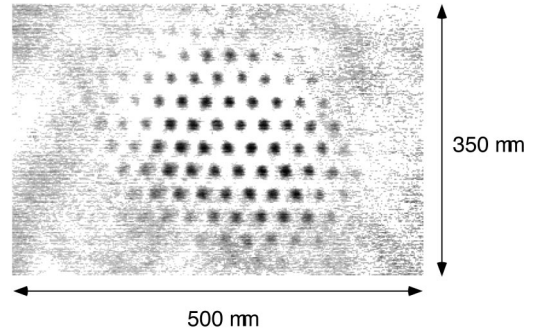


FIG. 3. Absorption image of atoms trapped in a far-detuned hexagonal lattice of period 29 μm . Each spot contains $\sim 10^4$ atoms.

each site the atoms form a vertical rod with a radial confinement of $\sigma_y = \sigma_z = 4.5(1.5)$ μm . The peak absorption coefficient is 20%. Each tube located near the center of the pattern contains about 10^4 atoms. This number remains almost constant up to a radius of 80 μm and then decreases because of the Gaussian spatial profile of the YAG beam. On the edges the potential depth is only on the order of the atomic temperature $\sim 2 - 5$ μK .

In this two-dimensional structure there are no vacancies, i.e., all sites are macroscopically occupied. By turning on the beam creating the lattice at variable delays, we find that it takes about 10 ms to fill this 2D structure. When the YAG beam alone is left on for a time longer than ~ 20 ms, the images vanish because the atoms fall along the tubes.

However, there is a periodic structure along x due to the Talbot effect [9], which, for high enough intensity, is able to compensate gravity. To understand the periodicity along the vertical axis, consider the interference pattern created by the zeroth-order beam propagating along x having a field amplitude A_0 and the first-order diffracted beams of amplitude A_j ($j = 1$ to 6) that propagate along a direction that makes the angle θ with Ox . The interfering structure is of the form $I = |A_0 e^{ikx} + \sum_j A_j e^{ik_x x + \mathbf{k}_\perp \cdot \mathbf{r}_\perp}|^2$, where $|k_x| = |k \cos \theta|$. The interference pattern is periodic along x with period $p_x = 2\lambda/\theta^2 = 1.2$ mm for small θ . More generally, the second-order beams also contribute by interfering with the zeroth-order and first-order beams, giving a periodic pattern with a more complex substructure.

We have produced such 3D traps with a YAG beam waist of $w_0 = 60$ μm on the grating. Absorption images of atoms trapped in this 3D potential are very similar to Fig. 3 with fewer occupied sites. The $1/e$ lifetime of this sample is 0.35 s. The temperature is measured by TOF along x and by TOF imaging along y and z after suddenly switching off the YAG beam. We find an isotropic temperature of $T = 10(3)$ μK . The radial oscillation frequency is 5(1) kHz more than 15 times larger than in the single beam trap and twice the recoil frequency at 852 nm (2 kHz). The measured radial rms size is 3.5 μm , a value close to our resolution limit of 2.5 μm . From the measured temperature and oscillation frequency, we make another determination of this size, 0.8 μm , well below our resolution. We have numerically calculated the 3D optical potential created by the phase grating and gravity. For 2.5 W the depth is $U_0/k_B \sim 400$ μK . Because of the limited vertical extension of the MOT cloud (300 μm), at-

oms cannot be trapped in more than one or two potential wells along x , and we deduce an equilibrium size along x of $\sigma_x \sim 20 \mu\text{m}$. From these data, we obtain a rough estimate of the atomic peak density, which, in each tube, is larger than $\sim 10^{13} \text{ atoms/cm}^3$ and corresponds to a phase-space density larger than $\sim 10^{-3}$. Note that this estimate is in agreement with Eq. (1), which gives $n = 5 \times 10^{13} \text{ atoms/cm}^3$ for $\Delta T \sim 5 \mu\text{K}$. Even if the density has a large uncertainty¹ because of the uncertainty on the size of the sample, this cylindrical geometry is very appealing for future experiments with high density. These include photonic band-gap studies,

¹This density could be independently measured by transferring quickly the atoms in $F=4$ and recording the lifetime of the sample which should be in the ms range with the known value of the spin-exchange relaxation rate of $\sim 10^{-11} \text{ cm}^3/\text{s}$ [10–12].

evaporative cooling in order to enhance the phase-space density, or collision studies.

As a last example of trapping in a far-detuned potential, we have recorded absorption images of atoms trapped in speckle light when the grating is replaced by a holographic speckle pattern imaged onto the MOT. The observed random distribution of potential sites and the wide distribution of sizes and shapes are a clear signature of the disordered light pattern. These devices open the way to the study of atom transport in periodic or disordered systems in the classical or quantum regime.

The authors wish to thank K. Amar, Y. Castin, C. Cohen-Tannoudji, J.-Y. Courtois, J. Dalibard, and P. Jacquot. This work has been supported by CNES, BNM, CNRS, Collège de France, NEDO (Japan), and TMR Contract No. FMRX-CT96-0002 of the E.U. Laboratoire Kastler Brossel is Unité de Recherche de l'Ecole Normale Supérieure et de l'Université Pierre et Marie Curie, associée au CNRS.

-
- [1] See, for instance, *Laser Manipulation of Atoms and Ions*, edited by E. Arimondo, W.D. Phillips, and F. Strumia (North-Holland, Amsterdam, 1992); C. Adams and E. Riis, *Prog. Quantum Electron.* **21**, 1 (1997).
 - [2] J. D. Miller, R. A. Cline, and D. J. Heinzen, *Phys. Rev. A* **47**, R4567 (1994).
 - [3] T. Takekoshi and R. Knize, *Opt. Lett.* **21**, 77 (1996).
 - [4] S. Friebe, C. D'Andrea, J. Walz, M. Weitz, and T. Hänsch, *Phys. Rev. A* **57**, R20 (1998).
 - [5] H. Lee, C. Adams, M. Kasevich, and S. Chu, *Phys. Rev. Lett.* **76**, 2658 (1996).
 - [6] A. Kuhn, H. Perrin, W. Hänsel, and C. Salomon, in *OSA TOPS on Ultracold Atoms and BEC*, edited by K. Burnett (Optical Society of America, Washington, D.C., 1996), Vol. 7, p. 58.
 - [7] D. L. Haycock, S. E. Hamman, G. Klose, and P. S. Jessen, *Phys. Rev. A* **55**, R3991 (1997).
 - [8] D. Boiron, A. Michaud, P. Lemonde, Y. Castin, C. Salomon, S. Weyers, K. Szymaniec, L. Cognet, and A. Clairon, *Phys. Rev. A* **53**, R3734 (1996); D. Boiron, C. Triché, D. R. Meacher, P. Verkerk, and G. Grynberg, *ibid.* **52**, R3425 (1995).
 - [9] H. F. Talbot, *Philos. Mag.* **9**, 401 (1836).
 - [10] M. H. Anderson, J. R. Ensher, M. R. Matthews, C. E. Wieman, and E. A. Cornell, *Science* **269**, 198 (1995).
 - [11] C. R. Monroe, E. A. Cornell, C. A. Sackett, C. J. Myatt, and C. E. Wieman, *Phys. Rev. Lett.* **70**, 414 (1992).
 - [12] J. Dalibard (private communication).